The Journal of Experimental Biology 206, 67-74
Published by The Company of Biologists 2004
doi:10.1242/jeb.00716

Biomechanics of ant adhesive pads: frictional forces are rate- and temperature-dependent

Walter Federle[1,*], Werner Baumgartner[2] and Bert Hölldobler[1]

[1]*Zoologie II, Biozentrum, Am Hubland, D-97074 Würzburg, Germany* and [2]*Institute of Anatomy and Cell Biology, University of Würzburg, Koellikerstrasse 6, D-97070 Würzburg, Germany*

*Author for correspondence (e-mail: wfederle@biozentrum.uni-wuerzburg.de)

Accepted 23 September 2003

Summary

Tarsal adhesive pads enable insects to hold on to smooth plant surfaces. Using a centrifuge technique, we tested whether a 'wet adhesion' model of a thin film of liquid secreted between the pad and the surface can explain adhesive and frictional forces in Asian Weaver ants (*Oecophylla smaragdina*).

When forces are acting parallel to the surface, pads in contact with the surface can slide smoothly. Force per unit pad contact area was strongly dependent on sliding velocity and temperature. Seemingly consistent with the effect of a thin liquid film in the contact zone, (1) frictional force linearly increased with sliding velocity, (2) the increment was greater at lower temperatures and (3) no temperature dependence was detected for low-rate perpendicular detachment forces. However, we observed a strong, temperature-independent static friction that was inconsistent with a fully lubricated contact. Static friction was too large to be explained by the contribution of other (sclerotized) body parts. Moreover, the rate-specific increase of shear stress strongly exceeded predictions derived from estimates of the adhesive liquid film's thickness and viscosity.

Both lines of evidence indicate that the adhesive secretion alone is insufficient to explain the observed forces and that direct interaction of the soft pad cuticle with the surface ('rubber friction') is involved.

Key words: friction, adhesion, attachment, tarsus, arolium, rubber friction, Asian Weaver ant, *Oecophylla smaragdina*.

Introduction

Many arthropods and vertebrates possess legs with adhesive pads (for a review, see Scherge and Gorb, 2001), which can provide attachment to smooth surfaces. Adhesive pads have to be rapidly detached during locomotion, so their surface contact must be highly dynamic and controllable. To run and climb on smooth plant surfaces, animals not only have to deal with perpendicular, but also with shear forces. For climbers on vertical surfaces, shear forces are required to counteract gravity. Moreover, when sprawled-posture animals stand upright or hang upside-down, their body weight generates lateral (shear) forces acting away from or toward the body, respectively.

In all insects studied to date adhesion is mediated by a thin film of liquid secretion between the pad and the surface (e.g. Walker et al., 1985; Attygalle et al., 2000; Jiao et al., 2000; Gorb, 2001; Vötsch et al., 2002; Federle et al., 2002). Experimental attempts to remove this fluid using solvent (in *Rhodnius prolixus*; Edwards and Tarkanian, 1970) or silica gel treatment (in *Aphis fabae*; Dixon et al., 1990) suggested that the pad secretion is essential for adhesion, but the observed effects are hard to separate from reduced adhesion due to pad desiccation (see Jiao et al., 2000). By measuring adhesive forces in pads of *Tettigonia viridissima*, Jiao et al. (2000) found an increase of adhesive force with the applied preload and concluded that the secretion is necessary, but not sufficient for adhesion. However, it is still unclear how the fluid affects the performance of attachment pads and their adhesive and frictional forces.

Let us assume a simple, hypothetical 'wet adhesion' model of a homogenous liquid film between a smooth pad and a smooth surface. The fluid's surface tension generates a static force perpendicular to the surface. Surface tension forces parallel to the surface due to contact angle hysteresis between the leading and the trailing edges of the meniscus are probably small (see Appendix). By contrast, forces due to viscosity can act in the normal and in the parallel direction, but are zero under static conditions. Based on these considerations, we can make the following predictions for attachment performance: (1) A fluid film should act as a lubricant leading to reduced friction. Thus, static friction should be small and pads should readily start sliding. (2) Sliding of the pad will shear the liquid film. Forces depend on the rate of shear so that friction should increase with sliding velocity. (3) As viscosity decreases much more strongly with temperature than surface tension, sliding friction should become smaller at higher temperatures, but static forces should be almost temperature-independent.

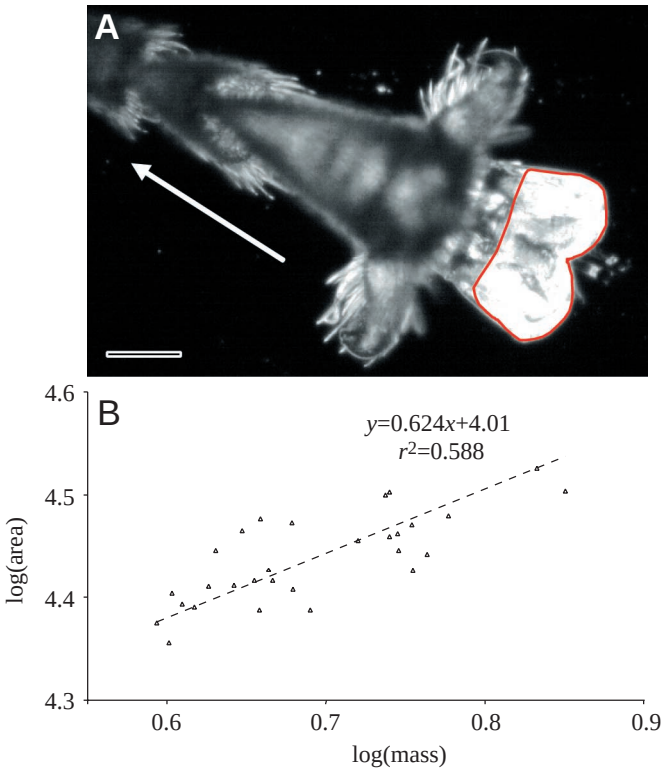

Fig. 1. (A) Measurement of contact area of the extended arolium in *O. smaragdina*. The arrow shows the sliding direction. Scale bar, 100 μm. (B) Scaling of pad contact area (mean of two hind legs, μm^2) with body mass (mg). A model II regression was performed.

So far, no data are available to test these predictions. It is unclear how insect attachment forces depend on sliding velocity and temperature. Only few studies have measured in-plane attachment performance of insect pads, and the results indicate that friction on smooth surfaces is relatively large (Stork, 1980; Gorb et al., 2001; Betz, 2002) and that friction forces are greater than adhesive forces (for blowflies; Walker et al., 1985). This contradicts the expected lubricating effect of the fluid film. Unfortunately, the data available represent either active pulling force (Stork, 1980; Betz, 2002) or detachment force measurements (Gorb et al., 2001), where it is unclear to what extent sliding was involved.

Here we investigate whether a simple 'wet adhesion' model is consistent with the frictional forces developed by an insect pad. By analyzing the sliding friction of *Oecophylla smaragdina* ants on a smooth turntable, we study how forces are related to sliding velocity and temperature.

Materials and methods

Study animals

Two colonies of *Oecophylla smaragdina* Fabr. were collected in West Malaysia and Brunei and kept in the laboratory. Ants were allowed to nest in glass tubes with moist cotton wool (as described in Hölldobler and Wilson, 1978) and were fed with honey-water and dead insects *ad libitum*. We gently collected individual workers from the nests with small paper strips and placed them in Petri dishes for the duration of the experiments.

Determination of body mass and arolium contact area

We weighed the ants to the nearest 0.01 mg and measured their hindleg arolium contact area. As the adhesive arolium in Hymenoptera is a highly dynamic, deployable organ (Federle et al., 2001), the pad contact area had to be measured in the unfolded position. Arolia partly in contact fully unfold when they are pulled across a smooth surface in the direction toward the body. We used this 'passive extension' reaction (Federle et al., 2001) to quantify pad contact area. Ants were held with fine tweezers and pulled across a microscope coverslip in the focus of a microscope under dark-field illumination. To facilitate imaging of the tarsi, we used a PCI 1000 B/W high-speed video camera (Redlake, San Diego, CA, USA) mounted on the microscope with a foot switch trigger. Contact area was measured from digital images (Fig. 1A). When fully unfolded, the contact area of the arolium of *Oecophylla smaragdina* is B-shaped (light area in Fig. 1A); the cuticle in this zone has a highly specialized fibrillar texture (see Federle et al., 2001). In *Oecophylla smaragdina*, arolia fully unfold with only moderate pulls (Federle et al., 2001). Our observations indicate that once unfolded, the arolium contact area remains largely constant, and that it is not or only weakly dependent on sliding velocity. Thus, the ratio of friction force and (maximum) contact area gives a reasonable estimate of the shear stresses acting during our sliding experiments. Contact area was measured twice for each hindleg and the mean values were used for further analysis.

Surface characterization using atomic force microscopy

We used atomic force microscopy (AFM) to measure the roughness of the experimental poly(methyl methacrylate) (PMMA; Plexiglas) surfaces. 100 μm × 100 μm topographic images were obtained using a Nanoscope III AFM (Digital Instruments, Mannheim, Germany). Surface roughness parameters were calculated from the height profile. Roughness was measured for fresh and used PMMA substrate (i.e. after use in the centrifuge and repeated cleaning). The fresh Plexiglas surfaces had a roughness average (R_a) of 0.548 nm (mean of three areas each 50 μm×50 μm). Cleaning the surface with lens cloth slightly increased surface roughness. For the used substrates, R_a was 3.429 nm (mean of three areas each 50 μm×50 μm).

Force measurement

To measure attachment forces of insects, we used a centrifuge technique similar to the method described by Federle et al. (2000). *O. smaragdina* ants were placed onto the smooth Plexiglas (PMMA) turntables (radius r=60 mm) or cylinders (r=40 mm) mounted in the rotor to measure friction or adhesive forces, respectively. Between experiments, the

Plexiglas surfaces were carefully cleaned with lens cloth and 25% ethanol. This treatment only slightly increased surface roughness (see above).

We simplified the experimental procedure of our previous study by using a strobe light synchronized to the revolutions of the centrifuge through a reflex photoelectric barrier so that a standing image of the insect on the rotating surface could be seen. The centrifuge was filmed from above (distance 0.9 m) with a standard 25 Hz CCD video camera (Panasonic F15) (instead of the previously used high-speed video system). Revolutions per minute (revs min^{-1}) of the centrifuge were recorded with an optical tachometer, the output voltage being displayed on a digital panelmeter attached to the transparent upper side of the centrifuge housing, so that the current speed of rotation was visible in the video image (Fig. 2A). We compared the tachometer readings with the values for revs min^{-1} obtained from a high-speed video recording and found perfect consistency.

In-plane (frictional) forces

Individual *O. smaragdina* ants were placed close to the center of the PMMA turntable and the centrifuge was accelerated until the ants stopped running. Once this 'freezing stage' (Federle et al., 2000) had been reached, acceleration of the centrifuge was continued very slowly. As soon as the insect started to slide, the centrifuge acceleration was stopped. Under these conditions, the ants did not detach from the turntable, but gradually slid outward to the edge of the turntable. The length of these 'slides' was 18–50 mm over a period of 20–140 s.

Apart from the centrifugal force $F_C=mr\omega^2$ (where m is body mass, r is radius, ω is angular velocity), the ants on the turntable experienced a lateral (tangential) force F_T. This force is acting against the direction of rotation and caused the ants to slide on slightly curved trajectories (Fig. 2A). It represents the sum of (1) the force due to the angular acceleration of the turntable $F_{Acc}=mr(d\omega/dt)$, (2) the Coreolis force $F_{Cor}=m\omega(dr/dt)$ and (3) air drag $F_{Drag}=0.5C_D\rho Av^2$, where C_D is the drag coefficient [in the range of Reynolds numbers reached here ($Re\approx10^4$), C_D is expected to be approximately 1 (Full and Koehl, 1993)], ρ is air density, v is velocity and A is the projected area of the ant in the radial plane. Forces due to angular acceleration and Coreolis force were calculated and found to be negligibly small (both force components were always <1 μN, never reaching more than 0.03% of the centrifugal force). The only significant tangential force comes from wind drag, and its contribution increases with radius. The projected area of an *Oecophylla smaragdina* worker was estimated as 15 mm^2 (measured from digitized, lateral images; N=10), and air density (at 200 m altitude) as 1.19 kg m^{-3} at 15°C and 1.13 kg m^{-3} at 30°C. Starting from these values, drag forces ranging from 3.5% (near the center of the turntable) to 6.8% (near the edge) of the current centrifugal force are expected. To evaluate this theoretical estimate of tangential forces, we calculated the expected deviation from a straight, radial trajectory by integrating tangential displacements (expressed as angles to the radius) over each run. The obtained result was compared with the actual tangential displacement of the ants over the whole run (measured using a paper template with marked radial sections attached under the transparent turntable; see Fig. 2A). Both angles were small and not significantly different (NS) from each other (expected deviation: 1.5±0.4°, observed deviation: 2.2±3.6°; paired t-test: P>0.1), which means that our above estimation of tangential forces is realistic.

The total force acting on the ant on the turntable is $F_{tot}=\sqrt{F_C^2+F_T^2}$. The ant's sliding velocity (on its curved trajectory) was calculated from measured radii by $v_{tot}=(F_{tot}/F_C)dr/dt$. Inclusion of tangential forces in the analysis increased the resulting forces (Figs 2 and 3) by less than 0.2%, so they had a negligible effect.

We analyzed the video recordings by measuring the ant's radius over the whole run in intervals of 2 s using Unimark 3.6 software (Rüdiger Voss Services, Tübingen, Germany). Data were analyzed in Matlab (The MathWorks, Inc.). To evaluate the relationship between force and sliding velocity, we performed model II (reduced major axis) regressions, because both variables are derived from the ant's radius, measured with error (Rayner, 1985; LaBarbera, 1989).

In a first set of experiments, intact *O. smaragdina* ants were tested on the PMMA turntable at 20°C and 25°C. In most cases, the sliding ants faced toward the outside of the turntable, the body held partly by the middle and primarily by the hind legs. The forces aligned the middle and hind legs parallel behind the body so that at the tarsi of these legs, the pull was acting in the direction toward the body. This condition helps to fully extend the arolia (Federle et al., 2001). However, the front legs (and partly the middle legs) behaved less regularly and often kept on moving while the other legs were in contact. Thus, the number of legs in contact varied and often changed during the runs. As a consequence, the forces were found to be variable.

To reduce this source of variation and to make possible a quantitative measurement of shear stress, we performed a second set of experiments, in which we removed the arolia of the middle and front legs. This operation was performed one day before the centrifuge experiments on anaesthetized ants using microscissors. The ants were allowed to recover individually in Petri dishes with sufficient humidity and fed with honey-water *ad libitum*. As a consequence of the treatment, all ants attained the same body orientation facing toward the outside of the turntable with the two hindlegs in contact (Fig. 2A).

Perpendicular detachment forces

As in our previous study (Federle et al., 2000), we measured the centrifugal force needed to detach ants from the outside of a smooth PMMA cylinder. Once the insect showed the 'freezing' reaction, we accelerated the centrifuge very slowly until it detached from the surface. The runs lasted for a period of 1–2 min. Centrifugal forces were calculated from the insect's radius and rotation speed at the moment of

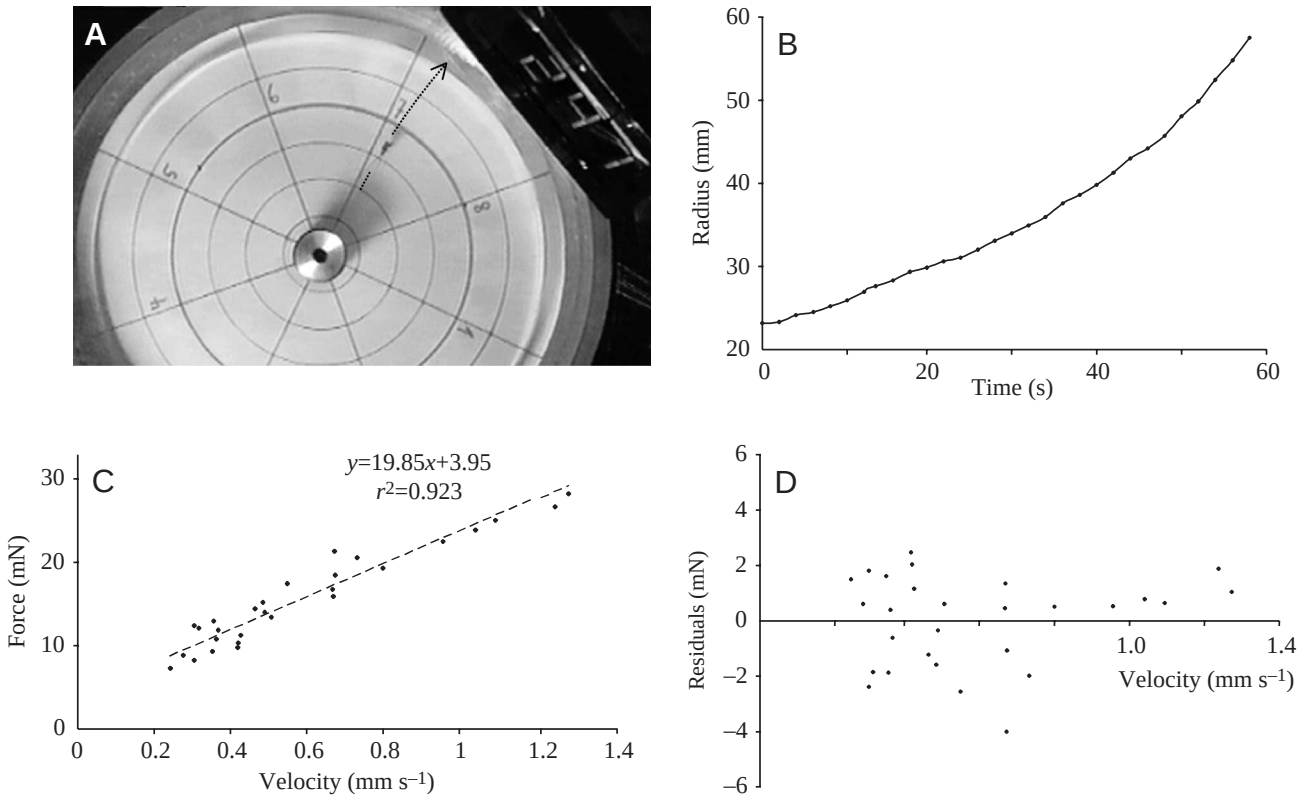

Fig. 2. (A) Video image of an *O. smaragdina* ant on the Plexiglas turntable rotating at 2470 revs min^{-1}. Dotted arrow shows the sliding trajectory. Note the two hindlegs in contact. (B) Gradual slide of *O. smaragdina* ant on a smooth turntable at 20°C. (C) Relationship between friction force and velocity for the data shown in B; model II regression. (D) Plot of regression residuals.

detachment. For each ant, we conducted three consecutive measurements and calculated its maximal attachment force. The ants were allowed to recover for at least 15 min between these three measurements.

Temperature dependence

Frictional and adhesive force measurements were conducted in a temperature- and humidity-controlled climatic chamber. Air humidity was kept constant at 50%. Friction forces with middle and front leg arolia removed were measured at 15 and 30°C. Perpendicular detachment forces were measured at 15, 20, 25 and 30°C. As several hours were required to change the room temperature, trials were performed on consecutive days using different ants.

Results

Velocity dependence of sliding friction

When strong shear forces were acting on *Oecophylla smaragdina* on the smooth turntable, the ants did not immediately detach, but gradually slid outward (Fig. 2A,B), their adhesive pads being in continuous contact with the surface. From the smooth radial sliding movements, we determined the relationship between force and sliding velocity, which strongly indicated a linear association (Fig. 2C). To test for a systematic deviation from linearity, we examined the residuals of the regression. No trends were detected (Fig. 2D). All the obtained model II regression lines (N=81) had positive intercepts (i.e. a force at zero velocity), indicating the presence of a static friction component (Fig. 2C).

In the first set of experiments (all arolia intact; T=20°C; N=13), we found a relationship between force and sliding velocity of $F=7.2+V\times16.5$ (in mN, where V is sliding velocity in mm s^{-1}), which corresponds to $F/W=188.2+V\times426.5$ expressed as force per body weight. Thus, *O. smaragdina* remained attached to the turntable even under extreme centrifugal forces as high as 600 times body weight. Detachment occurred in only 6 out of 13 ants at a mean force of 655 times body weight; the remaining ants were still in contact with the surface when they reached the edge of the turntable at an extreme mean force of 843 times body weight.

In the second set of experiments, the ants were sliding with just their hind legs in contact. In this condition, friction force per body weight at 15°C was still very large: $F/W=85.0+V\times196.6$. We calculated shear stress as the ratio of friction force and pad contact area of both hind legs. At 15°C, we found a relationship between shear stress and sliding velocity of $F/A=81.4+V\times181.1$ (mN mm^{-2}, where V is in mm s^{-1}, see Fig. 3). Detachment occurred in only 8 out of 25 runs (at a mean shear stress of 405.0 mN mm^{-2}); the other ants were still attached when they reached the edge of the turntable at a mean shear stress of 397.8 mN mm^{-2}.

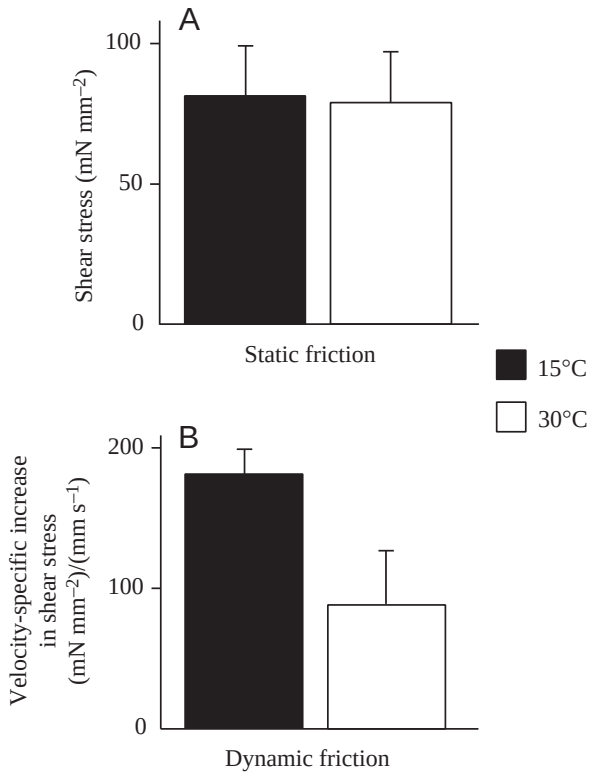

Fig. 3. Temperature dependence of static and dynamic friction in *O. smaragdina*. (A) Static shear stress. (B) Velocity-dependent increase of shear stress. Values are means ± S.D. of 13 ants at 15°C and 16 ants at 30°C (mean of 2 'slides' each).

Values of pad contact area were consistent with an isometric relationship ($A \propto m^{0.66}$). A logarithmic model II regression of hindleg contact area against body mass in *Oecophylla smaragdina* yielded a slope of 0.624 (Fig. 1B).

Temperature dependence of attachment forces

(a) Friction

We evaluated the relationship between shear stress and velocity for ants sliding at 15°C and 30°C. Fig. 3A shows that the static component did not differ between the temperatures (*t*-test; N_1=13, N_2=16; P>0.1). In contrast, the velocity-dependent component of friction showed a strong temperature dependence (Fig. 3B; *t*-test; N_1=13, N_2=16; P<0.001). The velocity-specific increment of shear stress at 15°C was 2.04 times greater than at 30°C.

(b) Perpendicular detachment forces

Similar to our findings for static friction, we did not detect any temperature dependence in low-rate perpendicular detachment forces over the range of the temperatures tested (15°C, 20°C, 25°C and 30°C) (analysis of covariance, ANCOVA), body mass as the covariate; $F_{3,54}$=0.3498; P>0.1, Fig. 4). Perpendicular detachment force at 20°C was 2.2 times smaller than the static friction component at the same temperature.

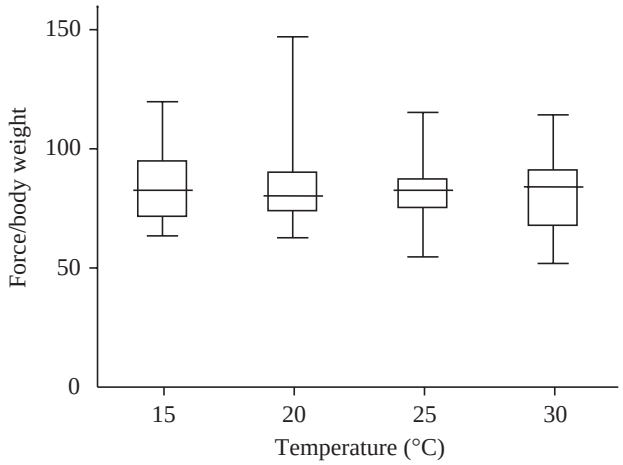

Fig. 4. Temperature dependence of perpendicular detachment forces in *O. smaragdina*. *N*=15 ants were tested at each temperature (maximum of three runs per ant). Central horizontal lines denote medians, boxes denote the inner two quartiles, and whiskers mark maxima and minima.

Discussion

The results presented here show that attachment performance in *Oecophylla smaragdina* on a smooth surface is strongly dependent on velocity and temperature. We find that friction forces consist of a static, temperature-independent part and a dynamic component sensitive to temperature. Our findings are not only important for understanding the performance of adhesive pads under natural conditions but also provide new insight into the general mechanism of surface adhesion in insects.

Performance of adhesive pads

Friction forces in *Oecophylla smaragdina* strongly increased with sliding velocity. Dynamic increase of attachment with velocity is probably a biologically important feature, enabling insects to reject rapid and strong perturbations (such as falling rain drops or wind gusts) without having to deal with excessive attachment forces during normal locomotion. In the Hymenoptera (and probably many other insects), reaction to perturbations can be entirely passive and has two components: (1) the unfolding of the adhesive pad and increase of the pad contact area (Federle et al., 2001) and (2) a velocity-specific increase of the friction force per unit contact area ('lateral tenacity'). In *Oecophylla smaragdina*, arolia completely unfold upon only moderate pulls (Federle et al., 2001) and before the pads begin to slide. In the experiments presented here, arolia were fully unfolded so that their contact area did not change considerably. Thus, our data support the velocity-dependence of lateral tenacity.

Given the ultrastructural similarity of the pad cuticle in different insect orders (Gorb, 2001; Gorb and Beutel, 2001), it is likely that our findings apply generally to insects with smooth adhesive pads. Velocity-dependent resistance to shear forces has also been demonstrated in adhesive pads of tree

frogs (Hanna and Barnes, 1991). To our knowledge, the only data on temperature dependence in tarsal adhesive pads are from geckos (Losos, 1990). Losos found a maximal attachment performance at approx. 20°C and concluded that clinging capability is related to temperature-dependent physiological and physical processes. The author interpreted poor clinging performance by reduced muscular activity at low temperatures, but by physical mechanisms at higher temperatures. The temperature dependence of sliding friction observed in our study is probably only based on physical effects. Because of the ants' freezing behavior in the centrifuge, forces were measured on virtually motionless ants with fully unfolded arolia. Thus, physiological effects probably did not play a significant role.

Friction forces in *Oecophylla smaragdina* were much larger than adhesive forces. The parallel, static component alone was 2.2× greater than the perpendicular detachment force (at the same temperature). As soon as the pads slide, frictional forces can be several times greater. Forces equivalent to as much as 1000 times body weight were still insufficient to detach the ants from the smooth turntable. Extreme attachment performance in *Oecophylla smaragdina* is probably related to the specialized leaf tent nest contruction behavior in this ant species (Wheeler, 1915; Hölldobler and Wilson, 1983). Ants start the construction of new nests by forcefully pulling together neighboring leaves, which are later connected with larval silk. While pulling, these ants are often standing on a smooth leaf upper side for hours and sustain large static forces parallel to the surface. More insect species need to be investigated to determine whether static friction is adaptive in this species or represents a general property of insect adhesive pads.

Wet adhesion or rubber friction?

The observed pad performance in *Oecophylla smaragdina* seems to be consistent with predictions derived from a wet adhesion model: (1) adhesive pads slide when subjected to shear forces on a smooth substrate; (2) there was a linear relationship between friction force and sliding velocity; (3) only the dynamic and not the static forces were temperature-dependent. However, the considerable magnitude of static friction clearly contradicts the proposed simple liquid film model. As shown in the Appendix, (static) friction forces due to surface tension are much too small to explain the observed static friction. Even though static friction was smaller than the forces reached during sliding, it corresponded to as much as 188.2 times body weight at 20°C and was by no means negligible.

To investigate whether this significant static friction could be caused by body parts other than the arolia (claws, tarsi), we make the (unrealistic) supposition that these parts are pressed down to the surface with the maximum adhesive force F_A (body parts are probably pressed down with a much smaller force to avoid the risk of arolium detachment). Even this conservative assumption leads to an estimated static friction coefficient at 20°C of $\mu_s = F_{Friction}/(F_{Weight}+F_A) \cong 2.2$. This estimate clearly exceeds typical values for the friction between rigid solids (e.g. friction coefficient of beetle cuticle on glass = 0.35; Dai et al., 2002). Thus, the large static friction cannot be explained by the contribution of other (sclerotized) body parts but probably involves a direct interaction of the 'rubbery' arolium cuticle with the surface.

Unlike rigid solids, which contact each other only at the highest tips of surface asperities, rubbery materials can deform to replicate the surface profile and achieve much larger real contact areas. We assume that the soft arolium cuticle behaves similarly. The results for thin water films trapped between rubber spheres and smooth glass (Roberts, 1971; Roberts and Tabor, 1971) showed that friction was mainly determined by the liquid's viscosity for film thicknesses of >7 nm. For thinner films, however, friction forces strongly increased. This enhanced friction can be related to the formation of dry contacts by dewetting of a metastable liquid film (e.g. Brochard-Wyart and de Gennes, 1994; Martin and Brochard-Wyart, 1998), or to solid-like behavior of the adhesive secretion due to non-Newtonian (viscoplastic, 'yield stress') properties of the fluid, or to molecular ordering of the liquid at zones where the film becomes thinner than approx. 10 monolayers (e.g. Granick, 1991; Raviv et al., 2001). Even if no dry or pinned solid contacts are formed, friction can also increase when surface asperities higher than the liquid film deform the rubber (Roberts, 1971). Considering the very small roughness of our experimental surfaces, this would mean that the film thickness locally decreases to values below 5 nm.

Not only the significant static friction but also the magnitude of the velocity-specific increment of friction indicate that the pad cuticle directly interacts with the surface. We estimated the height and viscosity of the adhesive liquid film using interference reflection microscopy (Federle et al., 2002; W.F., unpublished results). Assuming that the velocity-specific increase of friction is only due to shearing of the liquid film, our viscosity estimate of 40–150 mPa (at 25°C) and the observed velocity-specific increment of 89 (mN mm^{-2}/mm s^{-1}] at 30°C (Fig. 3B) would lead to a film thickness of not more than 1.7 nm. In this range, the sliding pad cuticle would be deformed by surface asperities, which contradicts our assumption above. Moreover, a film thickness of 1.7 nm is far below our interferometric measurements on pads in static contact (90–160 nm film thickness; Federle et al., 2002).

Static friction in rubber has been found to depend directly on contact area (Barquins and Roberts, 1986). The static shear stress of rubber reported in the study by Barquins and Roberts (250 kPa, on dry glass; Barquins and Roberts, 1986) is of the same order of magnitude but significantly larger than the static shear stress found in our study (ca. 80 kPa). The difference can easily be attributed to the presence of the liquid secretion. A 'rubber friction' model for the insect adhesive pad provides an explanation not only for the presence of a significant static friction, but also for the strong dependence on velocity and temperature. When viscoelastic rubber slides on a rough substrate, surface asperities of the substrate exert oscillating forces on the rubber surface leading to energy dissipation

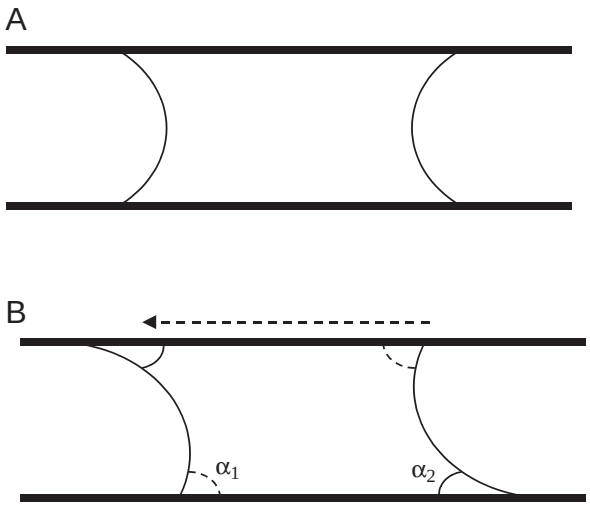

Fig. 5. Simple 'wet adhesion' model of insect adhesive contact. (A) Liquid film of constant height between the pad and the surface forming a meniscus. (B) When the pad slides (arrow), the meniscus is deformed, resulting in different contact angles α_1 and α_2 at the leading and trailing edges of the pad.

(internal friction) of the rubber (e.g. Grosch, 1963; Persson, 1998). In addition, rubber–substrate adhesion can also be important for friction (Persson, 1998). Rubber friction depends on the temperature-dependent complex elastic modulus $E\omega$ of the polymer and is maximal at the oscillation frequency ω, with the highest ratio between loss and storage modulus (Persson, 1998). For small sliding speeds (below this maximum), stick-slip behavior and Schallamach waves are absent and rubber friction typically increases with velocity, the increment being smaller at higher temperatures (Grosch, 1963; Persson 2001). Thus, all aspects of the ants' sliding behavior can be qualitatively explained by a rubber friction model. To test the validity of the 'rubber friction' model for insect adhesive pads, both the complex elastic modulus $E\omega$ of the pad cuticle material and its interaction with different surface profiles need to be characterized in further studies.

We wish to thank Friederike Haass for her assistance in the centrifuge experiments. Fruitful discussions with K. Autumn, E. L. Brainerd, R. J. Full, S. N. Gorb and T. A. McMahon are greatfully acknowledged. This study was financially supported by research grants of the Deutsche Forschungsgemeinschaft (SFB 567/A4, SFB 487/B5 and Emmy-Noether fellowship FE 547/1-1 to W.F.).

Appendix

Possible in-plane contribution of surface tension

Here we estimate to what extent surface tension could contribute to in-plane forces assuming a simple 'wet adhesion' model of a homogenous liquid film between the pad and the surface (Fig. 5A). When the pad slides on the surface, the contact angle of the adhesive liquid film on the surface becomes larger at the leading and smaller at the trailing edge (Fig. 5B). An expression for the resulting, retentive force is given by West (1911) for the similar case of a thread of mercury moving through a glass tube:

$$F = 2\pi r\gamma_L(\cos\alpha_1 - \cos\alpha_2)\,, \qquad \text{(A1)}$$

where $2\pi r$ is the inner perimeter of the tube, γ_L is the fluid's surface tension and α_1, α_2 are the leading and trailing edge contact angles, respectively. For simplicity, we model the contact area as a square (side length $2R$) and assume the contact angle deformation to be constant over the leading and trailing edges of the pad contact zone and to be independent of velocity. The in-plane force for one pad due to surface tension is then:

$$F = 4R\gamma_L(\cos\alpha_1 - \cos\alpha_2)\,, \qquad \text{(A2)}$$

where R is half the width of the pad contact area A (estimated here as $R=\sqrt{A/\pi}$). An analogous result is given by Extrand and Gent (1990) for the retention of liquid drops on solid surfaces. Using mean values for the contact area A (27500 μm^2) and an estimate of 30 mN m^{-1} for the surface tension γ_L of a mainly hydrophobic secretion (Israelachvili, 1992), we obtain:

$$F << 8R\gamma_L \approx 22\ \mu N \text{ (corresponding to approx. 0.8 mN mm}^{-2}\text{)}. \qquad \text{(A3)}$$

Even this maximal estimate is about 100 times smaller than the measured static shear stress. Thus, we conclude that surface tension plays a negligible role in frictional forces.

References

Attygalle, A. B., Aneshansley, D. J., Meinwald, J. and Eisner, T. (2000). Defense by foot adhesion in a chrysomelid beetle (*Hemisphaerota cyanea*): characterization of the adhesive oil. *Zoology* **103**, 1-6.

Barquins, M. and Roberts, A. D. (1986). Rubber friction variation with rate and temperature: some new observations. *J. Phys. D Appl. Phys.* **19**, 547-563.

Betz, O. (2002). Performance and adaptive value of tarsal morphology in rove beetles of the genus *Stenus* (Coleoptera, Staphylinidae). *J. Exp. Biol.* **205**, 1097-1113.

Brochard-Wyart, F. and de Gennes, P. G. (1994). Dewetting of a water film between a solid and a rubber. *J. Phys. Condens. Matter* **6**, A9-A12.

Dai, Z., Gorb, S. N. and Schwarz, U. (2002). Roughness-dependent friction force of the tarsal claw system in the beetle *Pachnoda marginata* (Coleoptera, Scarabaeidae). *J. Exp. Biol.* **205**, 2479-2488.

Dixon, A. F. G., Croghan, P. C. and Gowing, R. P. (1990). The mechanism by which aphids adhere to smooth surfaces. *J. Exp. Biol.* **152**, 243-253.

Edwards, J. S. and Tarkanian, M. (1970). The adhesive pads of Heteroptera: a re-examination. *Proc. R. Entomol. Soc. Lond. A* **45**, 1-5.

Extrand, C. W. and Gent, A. N. (1990). Retention of liquid drops by solid surfaces. *J. Colloid Interface Sci.* **138**, 431-442.

Federle, W., Brainerd, E. L., McMahon, T. A. and Hölldobler, B. (2001). Biomechanics of the movable pretarsal adhesive organ in ants and bees. *Proc. Natl. Acad. Sci. USA* **98**, 6215-6220.

Federle, W., Riehle, M., Curtis, A. S. G. and Full, R. J. (2002). An integrative study of insect adhesion: mechanics and wet adhesion of pretarsal pads in ants. *Integr. Comp. Biol.* **42**, 1100-1106.

Federle, W., Rohrseitz, K. and Hölldobler, B. (2000). Attachment forces of ants measured with a centrifuge: better 'wax-runners' have a poorer attachment to a smooth surface. *J. Exp. Biol.* **203**, 505-512.

Full, R. J. and Koehl, M. A. R. (1993). Drag and lift on running insects. *J. Exp. Biol.* **176**, 89-101.

Gorb, S. (2001). *Attachment Devices of Insect Cuticle*. Dordrecht, Boston: Kluwer Academic Publishers.

Gorb, S., Gorb, E. and Kastner, V. (2001). Scale effects on the attachment pads and friction forces in syrphid flies. *J. Exp. Biol.* **204**, 1421-1431.

Gorb, S. N. and Beutel, R. G. (2001). Evolution of locomotory attachment pads of hexapods. *Naturwissenschaften* **88**, 530-534.
Granick, S. (1991). Motions and relaxatons of confined liquids. *Science* **253**, 1374-1379.
Grosch, K. A. (1963). The relation between the friction and visco-elastic properties of rubber. *Proc. R. Soc. Lond. A* **274**, 21-39.
Hanna, G. and Barnes, W. J. P. (1991). Adhesion and detachment of the toe pads of tree frogs. *J. Exp. Biol.* **155**, 103-125.
Hölldobler, B. and Wilson, E. O. (1978). The multiple recruitment systems of the African weaver ant *Oecophylla longinoda* (Latreille) (Hymenoptera: Formicidae). *Behav. Ecol. Sociobiol.* **3**, 19-60.
Hölldobler, B. and Wilson, E. O. (1983). The evolution of communal nest-weaving in ants. *Am. Sci.* **71**, 490-499.
Israelachvili, J. (1992). *Intermolecular and Surface Forces*. London: Academic Press.
Jiao, Y., Gorb, S. and Scherge, M. (2000). Adhesion measured on the attachment pads of *Tettigonia viridissima* (Orthoptera, Insecta). *J. Exp. Biol.* **203**, 1887-1895.
LaBarbera, M. (1989). Analyzing body size as a factor in ecology and evolution. *Annu. Rev. Ecol. Syst.* **20**, 97-117.
Losos, J. B. (1990). Thermal sensitivity of sprinting and clinging performance in the Tokay Gecko (*Gecko gecko*). *Asiat. Herpetol. Res.* **3**, 54-59.
Martin, P. and Brochard-Wyart, F. (1998). Dewetting at soft interfaces. *Phys. Rev. Lett.* **80**, 3296-3299.
Persson, B. N. J. (1998). On the theory of rubber friction. *Surf. Sci.* **401**, 445-454.
Persson, B. N. J. (2001). Elastic instabilities at a sliding interface – art. no. 104101. *Phys. Rev. B* **63**, 104-101.
Raviv, U., Laurat, P. and Klein, J. (2001). Fluidity of water confined to subnanometre films. *Nature* **413**, 51-54.
Rayner, J. M. V. (1985). Linear relations in biomechanics: the statistics of scaling functions. *J. Zool. Lond. A* **206**, 415-439.
Roberts, A. D. (1971). The shear of thin liquid films. *J. Phys. D Appl. Phys.* **4**, 433-440.
Roberts, A. D. and Tabor, D. (1971). The extrusion of liquids between highly elastic solids. *Proc. R. Soc. Lond. A* **325**, 323-345.
Scherge, M. and Gorb, S. N. (2001). *Biological Micro- and Nanotribology: Nature's Solutions.* 304pp. Berlin, New York: Springer.
Stork, N. E. (1980). Experimental analysis of adhesion of *Chrysopolina polita* (Chrysomelidae: Coleoptera) on a variety of surfaces. *J. Exp. Biol.* **88**, 91-107.
Vötsch, W., Nicholson, G., Müller, R., Stierhof, Y.-D., Gorb, S. and Schwarz, U. (2002). Chemical composition of the attachment pad secretion of the locust *Locusta migratoria*. *Insect Biochem. Mol. Biol.* **32**, 1605-1613.
Walker, G., Yue, A. B. and Ratcliffe, J. (1985). The adhesive organ of the blowfly, *Calliphora vomitoria*: a functional approach (Diptera: Calliphoridae). *J. Zool. Lond. A* **205**, 297-307.
West, G. D. (1911). On the resistance to the motion of a thread of mercury in a glass tube. *Proc. R. Soc. Lond. A* **86**, 20-25.
Wheeler, W. M. (1915). On the presence and absence of cocoons among ants, the nest-spinning habits of the larvae and the significance of black cocoons among certain Australian species. *Ann. Entomol. Soc. Am.* **8**, 323-342.